HHS Public Access

Author manuscript

Mol Cell Neurosci. Author manuscript; available in PMC 2017 October 01.

Published in final edited form as:

Mol Cell Neurosci. 2016 October ; 76: 11–20. doi:10.1016/j.mcn.2016.08.002.

Early-life seizures alter synaptic calcium-permeable AMPA receptor function and plasticity

Jocelyn J. Lippman-Bell[1,2,*], **Chengwen Zhou**[2,*], **Hongyu Sun**[1,2], **Joel S. Feske**[2], and **Frances E. Jensen**[1,2]

[1]Perelman School of Medicine, University of Pennsylvania, Philadelphia, PA 19104

[2]Boston Children's Hospital, Boston, MA 02114

Abstract

Calcium (Ca^{2+})-mediated[1] signaling pathways are critical to synaptic plasticity. In adults, the NMDA glutamate receptor (NMDAR) represents a major route for activity-dependent synaptic Ca^{2+} entry. However, during neonatal development, when synaptic plasticity is high, many AMPA glutamate receptors (AMPARs) are also permeable to Ca^{2+} (CP-AMPAR) due to low GluA2 subunit expression, providing an additional route for activity- and glutamate-dependent Ca^{2+} influx and subsequent signaling. Therefore, altered hippocampal Ca^{2+} signaling may represent an age-specific pathogenic mechanism. We thus aimed to assess Ca^{2+} responses 48 hours after hypoxia-induced neonatal seizures (HS) in postnatal day (P)10 rats, a post-seizure time point at which we previously reported LTP attenuation. We found that Ca^{2+} responses were higher in brain slices from post-HS rats than in controls and this increase was CP-AMPAR-dependent. To determine whether synaptic CP-AMPAR expression was also altered post-HS, we assessed the expression of GluA2 at hippocampal synapses and the expression of long-term depression (LTD), which has been linked to the presence of synaptic GluA2. Here we report a decrease 48 hours after HS in synaptic GluA2 expression at synapses and LTD in hippocampal CA1. Given the potentially critical role of AMPAR trafficking in disease progression, we aimed to establish whether post-seizure *in vivo* AMPAR antagonist treatment prevented the enhanced Ca^{2+} responses, changes in GluA2 synaptic expression, and diminished LTD. We found that NBQX treatment prevents all three of these post-seizure consequences, further supporting a critical role for AMPARs as an age-specific therapeutic target.

[1]Abbreviations in abstract: Ca^{2+} = calcium, NMDAR = NMDA receptor, AMPAR = AMPA receptor, CP-AMPAR = Ca^{2+}-permeable AMPA receptor, LTD = long-term depression

Address correspondence to: Frances E. Jensen, MD, FACP, Professor and Chair, Department of Neurology, Perelman School of Medicine, University of Pennsylvania, 3400 Spruce Street, Philadelphia, PA 19104-4283, (215) 662-3360, frances.jensen@uphs.upenn.edu.

*JJ Lippman-Bell and C Zhou contributed equally to this work.

Current address for Dr. Lippman-Bell is Philadelphia College of Osteopathic Medicine, 4170 City Ave, Philadelphia, PA 19131, and for Dr. Zhou is Vanderbilt University Medical Center, 465 21st Ave South, Nashville, TN 37232-2551.

The authors declare that they have no conflict of interest.

Keywords

synaptic plasticity; epilepsy; neonate; glutamate receptor

Introduction

Calcium (Ca^{2+}) influx modulates critical activity-dependent molecular signaling pathways that regulate neuronal excitability, synaptogenesis, and synaptic plasticity (Graupner and Brunel, 2012; Ismailov et al., 2004; Malenka and Bear, 2004). Specific intracellular Ca^{2+} concentrations and dynamics are crucial determinants of synaptic plasticity (Ismailov et al., 2004; Lisman, 2001), and in adult hippocampal CA1, plasticity-related Ca^{2+} entry is largely attributed to influx through NMDARs. However, in the immature brain during peak synaptogenesis, Ca^{2+}-permeable AMPA receptors (CP-AMPARs) which lack the GluA2 subunit are expressed at relatively high levels compared to adults (Kumar et al., 2002; Pandey et al., 2015) providing an additional major route for Ca^{2+} entry (Burnashev et al., 1992; Isaac et al., 2007; Mammen et al., 1997; Pellegrini-Giampietro et al., 1992), and an additional mode by which glutamate could affect activity-dependent hippocampal synaptic plasticity.

During this developmental window of increased expression of CP-AMPARs, the brain is also highly susceptible to seizures, most commonly caused by hypoxic encephalopathy (Glass and Ferriero, 2007; Minchom et al., 1987; Silverstein and Jensen, 2007). Neonatal seizures often result in long-term disabilities, such as epilepsy and cognitive and behavioral deficits (Volpe et al., 2011; Wirrell et al., 2011). In P10 rats, hypoxia-induce seizures (HS) trigger later-life epilepsy and autistic-like social deficits (Lippman-Bell et al., 2013; Rakhade et al., 2011; Talos et al., 2012), as well as learning and cognitive deficits (Cha et al., 2002; Zhao et al., 2005). At the cellular and network levels, this may manifest as enhanced AMPAR function, with acute and chronic deficits in long-term potentiation (LTP) (Zhou et al., 2011). We previously showed that these behavioral and cellular consequences of HS can be reversed by post-treatment with AMPAR antagonists (Lippman-Bell et al., 2013). At the molecular level, HS at P10 induce rapid post-translational modification of AMPAR subunits, including the phosphorylation of Ser880 on the GluA2 subunit (Rakhade et al., 2008), which is consistent with GluA2 removal from the cell membrane (Isaac et al., 2007; Lin and Huganir, 2007; Rakhade et al., 2008). Thus, we hypothesized that the overall increase in AMPAR function following HS would be due largely to a synaptic increase in GluA2-lacking CP-AMPARs during brain development.

CP-AMPARs are most prevalent in normal immature brain and expression can be increased after seizures in development (Rakhade et al., 2008). Here, using combined immunohistochemistry, electrophysiology and Ca^{2+} imaging approaches, we found increased CP-AMPAR-mediated Ca^{2+} responses in hippocampal CA1 neurons at 48 hours after neonatal (P10) HS, temporally associated with decreased synaptic GluA2 expression associated with increased inwardly rectifying currents, a direct electrophysiological measure of the receptor Ca^{2+} permeability (Donevan and Rogawski, 1995; Kamboj et al., 1995; Koh et al., 1995; Washburn et al., 1997). In addition, long-term depression (LTD), a form of

plasticity dependent upon synaptic GluA2 expression (Dong et al., 2013; Fox et al., 2007; Isaac et al., 2007; Neyman and Manahan-Vaughan, 2008; Sanderson et al., 2016; Seidenman et al., 2003), also decreased 48 hours after HS at P10. Importantly, brief *in vivo* post-seizure treatment with the AMPAR antagonist 2,3-Dioxo-6-nitro-1,2,3,4-tetrahydrobenzo[*f*]quinoxaline-7-sulfonamide (NBQX) prevented the enhanced cellular Ca^{2+} responses, including the cellular response dependence on CP-AMPARs. NBQX also prevented the seizure-induced decreases in synaptic GluA2 expression, and the impaired LTD, further supporting a role for AMPARs in the genesis of these changes. Taken together, these results demonstrate a novel, age-specific mechanism leading to altered synaptic plasticity following neonatal seizures that can be targeted by early therapeutic intervention.

Methods

Animals

All studies were performed on litters of male Long–Evans rats (Charles River Laboratories, Wilmington, MA, 10 pups/litter). All procedures were approved by the Institutional Animal Care and Use Committees at Boston Children's Hospital (Boston, MA) and University of Pennsylvania (Philadelphia, PA), and are in accordance with the National Institutes of Health Guide for the Care and Use of Laboratory Animals. All efforts were made to minimize animal suffering and numbers.

Hypoxia-induced seizures

All rats weighing between 18 and 22 grams at P10 were randomly assigned as control or experimental and labeled with colored markers for identification. Rats in the experimental group were then subjected to HS, as described previously (Jensen et al., 1998). In brief, rats were placed in an airtight chamber (on a heating pad at 32–34°C), while 100% N_2 gas was infused to decrease ambient O_2 to 7, 5, and 4% for 8, 6, and 1 min, respectively. Tonic-clonic seizures were characterized by observed shaking throughout the body lasting longer than 5 seconds. Only rats demonstrating ≥5 tonic-clonic seizures during the 15 min hypoxia were included in the experimental group. All HS procedures were video-recorded to allow us to review them to confirm seizure number. Meanwhile, control rats were placed in an empty cage on a heating pad. All rats were away from their dam for the same amount of time and were returned to their home cage together.

Ratiometric Ca^{2+} imaging and analysis

Slices were prepared as for electrophysiology, then incubated at RT for 1 hour with 20–25μM Fura-2 AM (Invitrogen) plus 0.03% Pluronic F-127 (Invitrogen) to facilitate dye uptake and distribution, and subsequently washed in ACSF for >30min. For ratiometric imaging of Fura-2, slices were submerged in a recording chamber, allowing for laminar flow of oxygenated ACSF across the slice. Hippocampal CA1 was imaged using a 40× or 20×/0.50 Plan Fluor Ph1 DLL objective on a Nikon Eclipse TE2000-S inverted microscope with a Photometrics CoolSNAP-EZ interline CCD camera. Acquisition and analysis were performed using NisElements software (Nikon).

For each slice, baseline was recorded for 4 min. Next, kainic acid (KA) was bath applied (<2 min), then washed out for 10–15 min. For the antagonist experiments, after KA washout, 150μM of the CP-AMPAR blocker n-acetylspermine (NASP) (Koike et al., 1997; Tanaka et al., 2009), 100μM of the NMDA antagonist D-2-Amino-5-phosphonopentanoic acid (D-APV), or 20μM of the L-type voltage-gated Ca^{2+} channel blocker nimodipine was bath applied for 10 min, then KA in ACSF containing the antagonist was applied and washed out. Images were captured at 340nm and 380nm wavelength fluorescent illumination. During baseline and washout, images were collected at 25 sec intervals; during and after drug application, images were collected at 15 sec intervals. Any cells that did not exhibit full washout of Ca^{2+} signal 15 minutes of the KA removal were omitted from the study to avoid cell death artifacts. Cells that displayed Ca^{2+} flux or high baseline Ca^{2+} during collection of the baseline images were not included in the analysis.

To quantify the Ca^{2+} signal, time-lapse images were aligned and 340/380 ratios were measured within a region of interest (ROI) over CA1 pyramidal neuron somata. ROIs were determined by location (CA1 stratum pyramidale) and morphology (large, pyramidal-shaped) in both the bright field and baseline images and therefore blind to response magnitude. Background signal was subtracted using an additional ROI, then baseline ratio was subtracted from subsequent time points for each cell, providing the change in 340/380 fluorescence ratio from baseline. The peak 340/380 ratios from cells in each slice were averaged for analysis, thus n refers to number of slices, with 10–25 cells/slice. To determine significance, average peak 340/380 ratios were compared between groups by t-test or ANOVA if normally distributed, as assessed by D'Agostino and Pearson omnibus normality test, or tested by Mann-Whitney test or Kruskal-Wallis test if not normally distributed. If more than 1 slice was taken from the same animal, all data being compared were analyzed using repeated-measures ANOVA. To assess changes in Ca^{2+} response with NASP incubation in NQBX or vehicle-treated rats, one-sample t-test against a theoretical change of zero was used. To compare the change in response from baseline after drug application in the same slice, paired t-tests (response before vs. after drug) were used.

Synaptic GluA2 immunohistochemistry and image analysis

P12 rats were perfused transcardially with 4% paraformaldehyde. Brains were removed and post-fixed for 1hr, then saturated in 30% sucrose. Once saturated, brains were embedded in OCT, frozen, then cryosectioned at 40μm. Sections containing the middle 1/3 of the hippocampus were incubated without membrane permeabilization in a blocking solution of 10% normal goat serum (NGS) for 1 hour. Sections were incubated overnight at 4°C with an antibody directed against extracellular domain of GluA2 (1:500, Millipore, RRID: AB_2113875) (Danielson et al., 2012), washed in PBS, then incubated in AlexaFluor secondary (1:1000, Invitrogen) for 1 hour at room temperature (RT). Sections were then washed, permeabilized with 0.1% triton X, reblocked, and incubated with anti-synapsin (1:500, Millipore, RRID: AB_2200400), then AlexaFluor secondary (1:1000, Invitrogen), then mounted with Vectashield (Vector Labs). Sections incubated only with secondary antibody (no primary) were used to test antibody specificity. Surface specificity of the GluA2 antibody was confirmed in permeabilized and non-permeabilized sections incubated with an antibody to MAP2 (1:1000, Millipore, RRID: AB_805385), a protein that is

exclusively intracellular (Supplemental Fig 1), in addition to GluA2. MAP2 staining has been used previously as an indicator of membrane permeabilization and extracellular specificity of antibodies (Elmer et al., 2013; Glynn and McAllister, 2006). Blinded slides were imaged on a Zeiss LSM700 confocal microscope with an oil-immersion 63× 1.4 NA Plan-Apochromat objective for the control vs. post-HS set (described in Fig 2), or a Zeiss LSM710 confocal microscope with an oil-immersion 63× 1.7 NA objective for the NBQX treatment experiments (described in Fig 4). The z-interval for all stacks was 0.25μm. Because we aimed to assess extracellular GluA2, images were taken from CA1 stratum radiatum in the middle of the slice depth to avoid imaging cut membranes.

Three-dimensional image analysis of the collected z-stacks was performed blindly using Imaris software (Bitplane RRID: nif-0000-00314). To avoid a thresholding artifact, colocalization was first measured at the maximum threshold incorporating all GluA2 puncta, then the GluA2 channel was thresholded at multiple intervals of the max threshold (95, 90, 85, 80, 75, and 70%), and colocalization was determined again at each threshold (Nie et al., 2010; Zhou et al., 2011). After thresholding each channel, synapsin and GluA2 puncta were identified using the Imaris “spot” function. We next used the “spot co-localization” function, which links to a MatLab (RRID: nlx_153890) script that determines the proximity of two “spots”, allowing for determination of GluA2 puncta that “co-localized” with synapsin puncta (i.e. that were within the MatLab-determined proximity). The total number of colocalized punta was divided by volume (X*Y*Z planes), providing puncta/μm^3.

Electrophysiology

Control and HS rat pups were sacrificed at 48–72 hours post-seizures. Brains were quickly removed and acute 300μm coronal slices were prepared using a LEICA VT1000S vibratome (Leica Microsystem). Brains were submerged in a high-sucrose cutting solution containing (in mM): 210 Sucrose, 2.5 KCl, 1.02 NaH_2PO4, 0.5 $CaCl_2$, 10 $MgSO_4$, 26.19 $NaHCO_3$, and 10 D-glucose, pH 7.4, and bubbled with 95%O_2/5%CO_2 at 4°C. Slices were incubated at 32–34°C for 30min in artificial cerebral spinal fluid (ACSF) containing (in mM): 124 NaCl, 5 KCl, 1.25 NaH_2PO_4, 2 $CaCl_2$, 1.3 $MgSO_4$, 26 $NaHCO_3$, and 10 D-glucose, pH 7.4, as described previously (Zhou et al., 2011). Whole cell recordings were obtained from CA1 pyramidal neurons (Sanchez et al., 2001). To obtain rectification ratios, AMPAR-mediated EPSCs were elicited by stimulation of the Schaffer collaterals in ACSF containing picrotoxin (60μM) and DL-AP5 (100μM) to block $GABA_A$Rs and NMDARs, respectively, with the same intensity at holding potentials of −60 and 40 mV. All recordings were performed at RT (22–24°C). The serial resistance was monitored for stability (less than 10% change) during long recordings. Data were collected using an Axopatch 200B amplifier and Clampex 10.2 software.

To evoke LTD, two methods were used. First, extracellular field potentials (fEPSP) were recorded as previously described (Jensen et al., 1998; Zhou et al., 2011) at 30–32°C with no picrotoxin in the ACSF (Cummings et al., 1996; Okabe et al., 1998). Schaffer collaterals from CA3 to CA1 were stimulated at 30s intervals to obtain stimulus-response curves. Intensity (0.3 msec in duration) to evoke 60–70% maximal response was used as the test stimulus intensity. Low-frequency stimuli (LFS) for LTD induction consisted of 1800 shocks

at 2 Hz in 15 min. LTD was defined by a significant difference by paired t-test between baseline fEPSP slopes before LFS and at least 60 min after LFS (for one continuously 80 min recording) (Bolshakov and Siegelbaum, 1994; Oliet et al., 1997). Second, LTD was examined using whole cell patch clamp recordings with a pairing protocol (single cell, EPSC recordings) at RT (Cummings et al., 1996; Isaac et al., 1997; Okabe et al., 1998). LTD at this age (P12–13) could be induced in current-clamp mode (I=0) with 2 Hz stimuli (1800 shocks, 15 mins) in a modified ACSF (Ca^{2+}/Mg^{2+}=1) without picrotoxin and with potassium-based intracellular solution (Bolshakov and Siegelbaum, 1994; Oliet et al., 1997). LTD was defined by a significant difference by paired t-test between baseline EPSCs before and at least 30 min after pairing for one continuous 50 min recording (Bolshakov and Siegelbaum, 1994; Oliet et al., 1997).

In vivo drug administration

NBQX (2,3-dihydroxy-6-nitro-7-sulfamoyl-benzo[f]quinoxaline-2,3-dione, Sigma-Aldrich) was dissolved in 0.9% NaCl immediately prior to use. Control and HS rats were treated with NBQX (20 mg/kg i.p.; C+N, HS+N) or vehicle (C+V, and HS+V) immediately following hypoxia and every 12h for 3 additional injections (Koh et al., 2004). 20μm brain sections from each experimental group were stained, following manufacturer instructions, for with a 0.001% Fluoro-Jade B solution (Millipore) (Schmued and Hopkins, 2000) to test for degenerating neurons indicative of cell death.

Statistical analyses

Statistics were calculated using GraphPad Prism software. P values, n's, and means ± S.E. are reported throughout the results section. N refers to slices or image fields per treatment group unless otherwise noted.

Results

Seizures induce enhanced AMPAR-specific Ca^{2+} responses in CA1 neurons

Early-life seizures alter the activity of Ca^{2+}-dependent signaling molecules (Rakhade et al., 2008; Sanchez et al., 2005) and attenuate Ca^{2+}-dependent processes such as LTP in the hippocampus (Zhou et al., 2011). Therefore, we hypothesized that altered hippocampal Ca^{2+} signaling may represent an age-specific pathogenic mechanism for seizures occurring in a developmental window of high activity-dependent plasticity and synaptogenesis (Steward and Falk, 1991). To begin to test this, we assessed functional enhancement of Ca^{2+} responses in hippocampal CA1 neurons as visualized by Fura-2 ratiometric imaging in brain slices removed at 48 hours post-HS, a post-seizure time point at which we previously reported changes in AMPARs and an attenuation of LTP (Zhou et al., 2011) without evidence of cell death (Rakhade et al., 2011; Sanchez et al., 2001).

After recording a baseline Ca^{2+} response from CA1 neuron somata, we bath applied kainic acid (KA), a glutamate receptor agonist with a significantly higher affinity for AMPA and kainate glutamate receptors than for NMDARs (Hampson and Manalo, 1998). Because we hypothesized that HS would lead to increased Ca^{2+} influx, we used the lowest KA concentration needed to reliably evoke an unambiguous response in controls (2.5μM) to

allow us to measure the predicted post-HS increase without saturating Fura-2. The control responses were minimally detectable at this KA concentration, thus we repeated this experiment with 50μM KA to obtain larger responses and confirm that cells were loaded with Fura-2. At both the low and high KA concentrations, peak change in 340/380 ratio from baseline was significantly higher in cells from post-HS slices than in controls (post HS: mean response to 2.5μM KA=0.23±0.05, n=6 rats; response to 50μM KA=0.67±0.07, n=10 rats; controls: 2.5μM KA=0.12±0.02, n=6 rats, p=0.01 by repeated measures ANOVA, F=72.8; 50μM KA=0.51±0.07, n=10 rats p=0.049 by repeated measures ANOVA, F=7.8; Fig 1A–C). Ratio of peak 340/380 change from baseline in post-HS rats to that of littermate naïve controls was compared over multiple KA concentrations because post-HS:control response ratio versus KA concentration showed that the slope did not deviate from zero by linear regression analysis, indicating that seizures can alter AMPAR-mediated Ca^{2+} influx consistently and comparably across a range of concentrations from 2.5–50μM. All Ca^{2+} responses were reversible upon washout (Fig 1A). These data demonstrate that CA1 neurons respond to KA with a significantly larger rise in intracellular Ca^{2+} levels compared to controls, pointing to a pathologic state that could potentially alter Ca^{2+}-dependent processes in the cell.

Given that AMPAR activation by KA may cause a general depolarization that could subsequently activate multiple receptor types, we measured the specific contribution of CP-AMPARs to the Ca^{2+} response by incubating slices with CP-AMPAR blocker NASP. Ten-minute bath application of 150μM NASP lowered the post-HS Ca^{2+} response to the level of NASP-treated control slices, significantly decreasing the post-HS:control ratio (1.5±0.2 before and 0.9±0.1 after NASP; n=7 slices/group, p=0.02 by t-test, Fig 1A, D, E). Consistent with prior studies demonstrating that GluA2 is maturationally downregulated in early life (Pandey et al., 2015; Rozov et al., 2012; Sanchez et al., 2001), NASP decreased the Ca^{2+} response of control neurons in immature P12 hippocampal neurons (mean peak 340/380 difference from baseline=0.56 before and 0.35 after NASP; p=0.03 by paired t-test; n=7 slices from 5 rats; Fig 1A, D).

We next tested the contribution of NMDAR and voltage-gated Ca^{2+} channels to the Ca^{2+} response using bath application of NMDARs antagonist D-APV and the L-type Ca^{2+} channel blocker nimodipine. Although both D-APV and nimodipine significantly decreased the Ca^{2+}responses to KA, they did so by an equal magnitude in slices from post-HS and control rats. Therefore the Ca^{2+} response remained higher in post-HS slices than in control slices as reflected in the similar post-HS:control ratios before and after drug application (1.6±0.2 before and 1.8±0.2 after D-APV, n=6 slices/group, p=0.31 by t-test; 1.3±0.1 before and 1.4±0.2 after nimodipine, n=8 slices/group, p=0.44 by t-test; Fig 1E). Thus, only NASP eliminated the difference between post-HS and control response, accounting for the overall enhanced magnitude of Ca^{2+} response above control levels.

Seizures cause a decrease in synaptic GluA2 expression and an increase in AMPAR-mediated inward rectification in CA1 hippocampal neurons

We previously showed that HS at P10 increased GluR1 and AMPAR-mediated spontaneous EPSCs amplitude and frequency in CA1 48 hours post-HS (Sun et al., 2013; Zhou et al.,

2011), and that HS induced phosphorylation of hippocampal GluA2 receptors at Ser880 (Rakhade et al., 2008). Taken together with our current findings that the enhanced Ca^{2+} responses appear to be CP-AMPAR-mediated, we hypothesized that HS specifically increase the synaptic removal of GluA2 subunits, and therefore increase the expression of CP-AMPARs at the CA1 synapses. To evaluate synaptic GluA2 following HS, we performed double labeling for GluA2 using an antibody directed against the GluA2 extracellular domain (Danielson et al., 2012) and the presynaptic marker synapsin. Synaptic GluA2 expression (co-localized GluA2/synapsin puncta at 85% of max threshold) was significantly decreased in the stratum radiatum of hippocampal area CA1 at 48 hours post-HS compared to littermate naïve controls (post-HS animals: $1.0\pm0.2/\mu m^3$ for n=11 fields total from 6 rats; controls: $2.5\pm0.8/\mu m^3$ for n=8 fields from 5 rats; p=0.04 by t-test, Fig 2A–C). The significant difference between controls and post-HS rats persisted regardless of image threshold, indicating that changes were not an artifact of analysis parameters (Fig 2C; co-localization in seizure vs. control groups for all thresholds analyzed by 2-way ANOVA, p=0.0001, F=33.9; effect of threshold on seizure effect given as p=0.96, F=0.24), and was verified in all planes (Supplemental Fig 2). Assessing the level of dendritic GluA2, as measured by the presence of GluA2 within dendritic marker MAP2 labeling, indicated that total GluA2 levels increased, as opposed to only the ratio of GluA2 to synapsin (Supplemental Fig 3).

To physiologically confirm the decrease in synaptic GluA2, we examined the rectification ratios of AMPAR-mediated EPSCs (Kamboj et al., 1995; Washburn et al., 1997). Using whole-cell patch clamp recordings of CA1 neurons from slices removed at 48–72 hours post-seizure, we found an approximately 80% increase in the rectification ratio of AMPAR mediated EPSCs compared to neurons in slices from littermate controls (1.28±0.15 in control slices, n=5 cells from 3 rats, and 2.30±0.28 in post-HS slices, n=6 cells from 3 rats, p=0.014 by t-test; Fig 2D, E). Taken together with the immunohistochemical results, these data demonstrate a physiologically relevant decrease in GluA2 at synaptic AMPARs as early as 48 hours after seizures, in addition to rectification changes we found previously at 1 and 96 hours post-HS (Rakhade et al., 2008; Sanchez et al., 2001).

Impairment of long-term depression (LTD) in CA1 following early-life seizures

Ca^{2+} influx regulates synaptic plasticity (Ismailov et al., 2004; Lisman, 2001) and the synaptic presence of GluA2 is critical for the expression of the synaptic plasticity of LTD (Isaac et al., 2007; Malenka and Bear, 2004; Sanderson et al., 2016; Seidenman et al., 2003), where removal of GluA2 from the membrane results in impaired LTD (Seidenman et al., 2003). Because synaptic GluA2 decreased 48 hours after P10 HS, we next investigated whether LTD was compromised at this time point. Using an LTD pairing protocol to measure evoked EPSCs (eEPSCs) with whole-cell recordings (Isaac et al., 1996; Stevens and Wang, 1994) in CA1, we found that LTD was indeed impaired (control eEPSC amplitude percentage after LTD pairing: 61.9±3.2%, n=6 slices; and hypoxia eEPSC amplitude percentage after LTD pairing: 109.8±3.2%, n=6 slices; p=0.02 by t-test; Fig 3A, B). Extracellular field recordings confirmed that both control and post-HS slices showed evidence of LTD following low-frequency stimuli (LFS; 2 Hz, 1800 shocks, 15 min; p<0.001 for both control and post-HS slices by paired t-test of pre- vs. post-LFS; Fig. 3C),

the slope was significantly lower in control slices than in post-HS slices (control= −66.0±12.9%, n=5; post-HS=−20.47±3.13%, n=6; p=0.006, t-test; Fig. 3C, E).

Seizure-induced synaptic GluA2 changes can be prevented by post-HS treatment with the AMPAR antagonist NBQX

In vivo NBQX treatment (20mg/kg, i.p. immediately and 12, 24, and 36 hours post-HS) prevents post-HS attenuation of LTP (Zhou et al., 2011). Therefore, we tested whether the same treatment paradigm can prevent the enhanced Ca^{2+} response and rectification ratio, decreased synaptic GluA2 expression, and attenuated LTD observed at 48 hours post-HS.

NBQX treatment prevented the enhancement of Ca^{2+} responses. Compared to slices taken from littermate post-HS rats treated with vehicle (HS+V), slices from NBQX treated animals had significant reductions in Ca^{2+} response to 25uM KA in slices removed 48 hours post-HS (HS+V mean peak change in 340/380 ratio from baseline=0.44±0.05, median=0.41, n=11 slices from 8 rats/group; HS+N mean =0.27±0.03, median=0.30, p=0.01 by Mann Whitney test; Fig. 4A, B). As in Figure 1, we next measured Ca^{2+} responses evoked by KA from post-HS rats treated with NBQX (HS+N) or vehicle (HS+V) in the presence of the specific CP-AMPAR antagonist NASP to determine if these changes were specific to the CP-AMPARs. In the HS+V rats, incubation with NASP significantly lowered the neuronal Ca^{2+} response to KA, indicating a strong effect of NASP (−30.1±2.5%, p<0.0001 by one-sample t-test; n=6 slices from 4 animals; 8–19 cells/slice, Fig. 4A, C). However, following *in vivo* NBQX treatment, NASP did not significantly alter the Ca^{2+} response to KA (2.7±9.8%, p=0.79 by one-sample t-test; n=6 slices from 4 animals/group; 10–26 cells/slice, Fig. 4A, C), suggesting that the *in vivo* NBQX treatment paradigm effectively reduced the excessive CP-AMPAR function. Rectification ratios in adjacent slices were measured to confirm that the *in vivo* NBQX treatment prevented the post-seizure increase in CP-AMPAR function. Indeed we observed reduced rectification following NBQX (HS+V rectification ratio=2.57±0.2, n=8 slices; HS+N rectification ratio=1.69±0.3, n=7 slices, p=0.024 by t-test; Fig 4D). Further, neither the seizures nor the NBQX treatment caused cell death in CA1 by 48rs post-HS, as determined by Fluoro-Jade B staining (Supplemental Figure 4), consistent with publications showing that AMPARs do not increase constitutive neuronal death during early development (Aujla et al., 2009), in contrast to NMDARs (Ikonomidou et al., 1999; Manning et al., 2011). These data support our findings that *in vivo* NBQX treatment during the first 48 hours post-HS diminishes CP-AMPARs activity.

In addition to preventing the enhancement of Ca^{2+} responses, NBQX treatment *in vivo* prevented the post-HS decrease in synaptic GluA2 expression. GluA2/synapsin co-localization significantly increased in HS+N rats compared to HS+V littermates (HS+N: mean co-localized puncta at 85% of max threshold=6.61±0.4μm^3; HS+V, mean=4.98±0.4μm^3; at each threshold, p=0.0007 and F=6.91 by ANOVA for all 4 groups; with Bonferroni post-hoc test, p<0.05 for HS+V vs. HS+N; n=14 fields overall from 6 rats for each treatment group; Fig 4G, F). Furthermore, 48 hours of NBQX treatment began to normalize colocalization of GluA2 and synapsin levels in HS+N rats, as there were no significant differences compared to littermate controls treated with vehicle (C+V, 7.43±0.5μm^3; p>0.05 by post-hoc test for C+V vs. HS+N, n=11 fields overall from 5 C+V

rats, Fig 4F,G), although a slight decrease in GluA2/synapsin colocalization remained. Importantly, NBQX treatment in normal control littermates had no effect on GluA2 surface expression (C+N, 7.71±0.5μm^3; p>0.05 by post-hoc test for C+V vs. C+N, n=7 fields overall from 4 C+N rats, Fig 4G), demonstrating potential safety of this treatment paradigm. Consistent with the baseline experiments (Figure 1), there was no effect of analysis threshold (2-way ANOVA effect of threshold on treatment effect, p=0.74, F=0.59).

Finally, we asked whether NBQX also prevented the LTD deficit. Unlike slices from HS+V rats that showed impaired LTD, slices taken from CA1 of HS+N rats showed similar LTD to controls (−54.49±4.13%, n=8, t-test of HS+N vs. control LTD p=0.331, t-test vs. HS+V p<0.0001; Fig.4E). Thus, early seizure-induced changes in AMPARs and associated alterations in LTD plasticity can be prevented by early AMPAR blockade with NBQX.

Discussion

Here we showed that during a developmental window of extremely high activity-dependent plasticity and synaptogenesis (Steward and Falk, 1991), neonatal seizures increase neuronal AMPAR-dependent Ca^{2+} responses, decrease synaptic GluA2 expression in CA1 hippocampal neurons, and limit LTD expression. Moreover, the attenuation of the seizure-induced changes through post-seizure treatment with AMPAR antagonist NBQX supports a critical role for AMPARs as a potential age-specific therapeutic target to prevent early-life seizure-induced disruptions of normal development and synaptic plasticity.

Given the linkage between Ca^{2+} dynamics and plasticity in normal brain function, we sought to understand whether seizures alter Ca^{2+} influx through AMPARs in the highly plastic period of early brain development. Our results are the first to document Ca^{2+} dynamics alteration accompanying attenuated LTD in an early-life epilepsy model previously shown not to induce cell death (Rakhade et al., 2011; Sanchez et al., 2001). Changes in Ca^{2+} influx following seizures have been shown in SE models (Friedman et al., 2008; Rajasekaran et al., 2012), however SE models can induce cell death, thus the SE studies could not resolve whether changes in Ca^{2+} permeability were a product of excitotoxicity pathways or of epileptogenesis pathways. Our study confirms prior reports of altered post-seizure neuronal Ca^{2+} responses, supporting the idea that these changes are unlikely to be due to cell death (Rakhade et al., 2011) but are instead a conserved mechanism that could contribute to seizure-induced changes in neuronal function in multiple models.

In addition to early-life seizures, baseline levels and temporal fluctuations of intracellular Ca^{2+} are important for multiple forms of neuronal plasticity (Isaac et al., 2007; Malenka et al., 1989; Man, 2011; Turrigiano, 2012). Here, we showed that NASP, a selective channel-blocker of CP-AMPARs (Tsubokawa et al., 1995), but not blockers of NMDARs or L-type Ca^{2+} channels, prevented seizure-induced increases in Ca^{2+} responses in hippocampal slices, indicating that the excessive response was due primarily to CP-AMPARs. The route through which Ca^{2+} enters the cell upon stimulation can affect the magnitude and kinetics of Ca^{2+} entry, which can subsequently regulate plasticity (Graupner and Brunel, 2012; Ismailov et al., 2004; Yang et al., 1999; Yang et al., 2010). Specifically, a brief, high intracellular Ca^{2+} elevation results in LTP, whereas a sustained, low Ca^{2+} elevation leads to LTD (Castellani et

al., 2005; Lisman, 2001; Shouval et al., 2002; Yang et al., 1999). Enhanced activation of CP-AMPARs following HS would likely rapidly increase Ca^{2+} influx, perhaps shifting the optimal Ca^{2+} dynamics above the range favoring LTD, though not high enough to reach levels favoring LTP (Li et al., 2012). Along these lines, we have previously shown that early life seizures can also occlude LTP (Zhou et al., 2011). Hence, early-life seizures may create an intermediate Ca^{2+} range similar to the so-called “no-man’s land” (Cho et al., 2001; Lisman, 2001) at which point neither form of Hebbian plasticity mechanisms can be induced.

In addition to the evidence described above indicating that Ca^{2+} influx crucially regulates synaptic plasticity, synaptic localization of GluA2-lacking CP-AMPARs may be critical to the expression of hippocampal LTD (Isaac et al., 2007; Malenka and Bear, 2004; Sanderson et al., 2016; Seidenman et al., 2003). The changes in synaptic localization of CP-AMPARs required for LTD also occur following HS at P10. For example, removal of GluA2-containing AMPARs from synapses can occur through phosphorylation of GluA2 Ser880 (Seidenman et al., 2003), which increases in the hippocampus immediately post-HS (Rakhade et al., 2008). Further, insertion of GluA2-lacking CP-AMPARs during LTD is mediated by PKA and calcineurin activity and phosphorylation of GluA1 Ser845 (Sanderson et al., 2016), all of which acutely increase after HS at P10 (Rakhade et al., 2008; Sanchez et al., 2005).

The overlap in molecular mechanisms required for LTD with the molecular changes that acutely follow early-life HS raise the idea that early-life seizures may co-opt the baseline heightened state of plasticity in the developing brain. Our treatment data indicate that this may occur through alterations of highly plastic AMPARs that subsequently change Ca^{2+} responses and disrupt synaptic function. Specifically, early blockade of AMPARs *in vivo* with NBQX prevented both the seizure-induced increase in CP-AMPAR function, as demonstrated using measurements of inward rectification and NASP-dependent Ca^{2+} responses in adjacent slices from the same animals, as well as the attenuated LTD. Though additional mechanisms are likely to be involved, the summation of our data reported here and in prior reports indicates that blocking the initial overactivation of AMPARs is sufficient to stop secondary post-HS changes, including the Ca^{2+} and LTD changes reported here, neuronal hyperexcitability (Rakhade et al., 2008), occlusion of LTP (Zhou et al., 2011), long-term development of spontaneous recurrent seizures and deficits in social behavior (Lippman-Bell et al., 2013). Further, the efficacy of NBQX treatment in the first 48 hours also suggests that there is an early time point in the progression to epileptogenesis seen in this model that is mediated by activation of CP-AMPARs. Thus, there may be value in examining other Ca^{2+}-activated signaling cascades downstream from CP-AMPARs to better understand the dysplasticity related to early-life seizures.

Regulation of CP-AMPARs may represent an age-specific mechanism of epileptogenesis. The developing brain may be more vulnerable to the effects of seizure-induced changes as they target mechanisms that underlie synaptic and neuronal circuit development (Bassani et al., 2013; Yuan and Bellone, 2013). CP-AMPARs are important for early brain development and are expressed at higher baseline levels in the immature brain than in the adult (Kumar et al., 2002; Pandey et al., 2015). Their importance in the immature brain is highlighted in the

current study by the ability of NASP to strongly decrease Ca^{2+} responses even in slices from control P10 rats. However, recent reports indicate that inward rectification of AMPAR-mediated currents can also increase following adult status epilepticus (SE) (Rajasekaran et al., 2012), albeit to a lesser extent. Hence, seizure-induced conversion of AMPARs to CP-AMPARs may also be relevant to epilepsy in the adult as well as the immature brain. Finally, post-seizure rescue of published outcome measures by NBQX treatment appears to be specific to early-life seizures, as a recent study found that NBQX does not have anti-epileptogenic effects in adults (Twele et al., 2015). Therefore, the mechanism described in this report appears to be particularly sensitive in the P10 time window (developmentally similar to humans at term), providing an essential piece of preclinical information to guide the development of specific treatment options.

Conclusions

Taken together, the current study offers mechanistic insight into our prior work showing indirect evidence of altered Ca^{2+}-influx and GluA2 down-regulation (Rakhade et al., 2008; Sanchez et al., 2001) by demonstrating decreased synaptic GluA2 at the same post-seizure time point as functional cellular changes. Importantly, we obtained these results under identical conditions to our prior work where early-life HS induces long-term disruptions in synaptic plasticity, epilepsy, and behavior (Lippman-Bell et al., 2013; Talos et al., 2012), implicating modulation of synaptic CP-AMPARs as an age-specific, modifiable factor critical to the effects of early-life seizures on developing networks. Hence, treatments that target transient CP-AMPAR activation represent an age-specific therapeutic strategy for consideration clinically in the setting of neonatal seizures. Our results suggest that there may be value in examining other Ca^{2+}-activated signaling cascades downstream from CP-AMPARs to better understand the dysplasticity related to early-life seizures.

Supplementary Material

Refer to Web version on PubMed Central for supplementary material.

Acknowledgments

We thank Peter Klein, Marcus Handy, Leah Jacobs, and Samantha Soldan for technical assistance, Haochang Shou for statistical consultation, and Marc Dichter, Delia Talos, Yeri Song, and Ramani Balu for helpful comments on the manuscript. This work was supported by National Institutes of Health Grants NS 068161 (JJL), NS 031718 (FEJ), DP1 OD003347 (FEJ) (from the Office of the Director), and core support from the Intellectual and Developmental Disorders Research Center Grant (NIH NICHHD P30 HD18655).

References

Aujla PK, Fetell MR, Jensen FE. Talampanel suppresses the acute and chronic effects of seizures in a rodent neonatal seizure model. Epilepsia. 2009; 50:694–701. [PubMed: 19220413]

Bassani S, Folci A, Zapata J, Passafaro M. AMPAR trafficking in synapse maturation and plasticity. Cell Mol Life Sci. 2013; 70:4411–4430. [PubMed: 23475111]

Bolshakov VY, Siegelbaum SA. Postsynaptic induction and presynaptic expression of hippocampal long-term depression. Science. 1994; 264:1148–1152. [PubMed: 7909958]

Burnashev N, Monyer H, Seeburg PH, Sakmann B. Divalent ion permeability of AMPA receptor channels is dominated by the edited form of a single subunit. Neuron. 1992; 8:189–198. [PubMed: 1370372]

Castellani GC, Quinlan EM, Bersani F, Cooper LN, Shouval HZ. A model of bidirectional synaptic plasticity: from signaling network to channel conductance. Learn Mem. 2005; 12:423–432. [PubMed: 16027175]

Cha BH, Silveira DC, Liu X, Hu Y, Holmes GL. Effect of topiramate following recurrent and prolonged seizures during early development. Epilepsy Res. 2002; 51:217–232. [PubMed: 12399072]

Cho K, Aggleton JP, Brown MW, Bashir ZI. An experimental test of the role of postsynaptic calcium levels in determining synaptic strength using perirhinal cortex of rat. J Physiol. 2001; 532:459–466. [PubMed: 11306664]

Cummings JA, Mulkey RM, Nicoll RA, Malenka RC. Ca2+ signaling requirements for long-term depression in the hippocampus. Neuron. 1996; 16:825–833. [PubMed: 8608000]

Danielson E, Metallo J, Lee SH. Role of TARP interaction in S-SCAM-mediated regulation of AMPA receptors. Channels (Austin). 2012; 6:393–397. [PubMed: 22878254]

Donevan SD, Rogawski MA. Intracellular polyamines mediate inward rectification of Ca(2+)-permeable alpha-amino-3-hydroxy-5-methyl-4-isoxazolepropionic acid receptors. Proc. Natl. Acad. Sci. U. S. A. 1995; 92:9298–9302. [PubMed: 7568121]

Dong Z, Bai Y, et al. Hippocampal long-term depression mediates spatial reversal learning in the Morris water maze. Neuropharmacology. 2013; 64:65–73. [PubMed: 22732443]

Elmer BM, Estes ML, Barrow SL, McAllister AK. MHCI requires MEF2 transcription factors to negatively regulate synapse density during development and in disease. J Neurosci. 2013; 33:13791–13804. [PubMed: 23966700]

Fox CJ, Russell K, Titterness AK, Wang YT, Christie BR. Tyrosine phosphorylation of the GluR2 subunit is required for long-term depression of synaptic efficacy in young animals in vivo. Hippocampus. 2007; 17:600–605. [PubMed: 17534972]

Friedman LK, Saghyan A, Peinado A, Keesey R. Age- and region-dependent patterns of Ca2+ accumulations following status epilepticus. Int J Dev Neurosci. 2008; 26:779–790. [PubMed: 18687397]

Glass HC, Ferriero DM. Treatment of hypoxic-ischemic encephalopathy in newborns. Curr Treat Options Neurol. 2007; 9:414–423. [PubMed: 18173941]

Glynn MW, McAllister AK. Immunocytochemistry and quantification of protein colocalization in cultured neurons. Nat Protoc. 2006; 1:1287–1296. [PubMed: 17406413]

Graupner M, Brunel N. Calcium-based plasticity model explains sensitivity of synaptic changes to spike pattern, rate, and dendritic location. Proc Natl Acad Sci U S A. 2012; 109:3991–3996. [PubMed: 22357758]

Hampson DR, Manalo JL. The activation of glutamate receptors by kainic acid and domoic acid. Nat Toxins. 1998; 6:153–158. [PubMed: 10223631]

Ikonomidou C, Bosch F, et al. Blockade of NMDA receptors and apoptotic neurodegeneration in the developing brain. Science. 1999; 283:70–74. [PubMed: 9872743]

Isaac JT, Ashby M, McBain CJ. The role of the GluR2 subunit in AMPA receptor function and synaptic plasticity. Neuron. 2007; 54:859–871. [PubMed: 17582328]

Isaac JT, Crair MC, Nicoll RA, Malenka RC. Silent synapses during development of thalamocortical inputs. Neuron. 1997; 18:269–280. [PubMed: 9052797]

Isaac JT, Hjelmstad GO, Nicoll RA, Malenka RC. Long-term potentiation at single fiber inputs to hippocampal CA1 pyramidal cells. Proc. Natl. Acad. Sci. U. S. A. 1996; 93:8710–8715. [PubMed: 8710936]

Ismailov I, Kalikulov D, Inoue T, Friedlander MJ. The kinetic profile of intracellular calcium predicts long-term potentiation and long-term depression. J Neurosci. 2004; 24:9847–9861. [PubMed: 15525769]

Jensen FE, Wang C, Stafstrom CE, Liu Z, Geary C, Stevens MC. Acute and chronic increases in excitability in rat hippocampal slices after perinatal hypoxia in vivo. J. Neurophysiol. 1998; 79:73–81. [PubMed: 9425178]

Kamboj SK, Swanson GT, Cull-Candy SG. Intracellular spermine confers rectification on rat calcium-permeable AMPA and kainate receptors. J Physiol. 1995; 486(Pt 2):297–303. [PubMed: 7473197]

Koh DS, Burnashev N, Jonas P. Block of native Ca 2+ -permeable AMPA receptors in rat brain by intracellular polyamines generates double rectification. Journal of Physiology. 1995; 486.2:305–312. [PubMed: 7473198]

Koh S, Tibayan F, Simpson J, Jensen F. NBQX or topiramate treatment after perinatal hypoxia-induced seizures prevents later increases in seizure-induced neuronal injury. Epilepsia. 2004; 45:569–575. [PubMed: 15144420]

Koike M, Iino M, Ozawa S. Blocking effect of 1-naphthyl acetyl spermine on Ca(2+)-permeable AMPA receptors in cultured rat hippocampal neurons. Neurosci Res. 1997; 29:27–36. [PubMed: 9293490]

Kumar SS, Bacci A, Kharazia V, Huguenard JR. A developmental switch of AMPA receptor subunits in neocortical pyramidal neurons. J. Neurosci. 2002; 22:3005–3015. [PubMed: 11943803]

Li L, Stefan MI, Le Novere N. Calcium input frequency, duration and amplitude differentially modulate the relative activation of calcineurin and CaMKII. PLoS One. 2012; 7:e43810. [PubMed: 22962589]

Lin DT, Huganir RL. PICK1 and phosphorylation of the glutamate receptor 2 (GluR2) AMPA receptor subunit regulates GluR2 recycling after NMDA receptor-induced internalization. J Neurosci. 2007; 27:13903–13908. [PubMed: 18077702]

Lippman-Bell JJ, Rakhade SN, Klein PM, Obeid M, Jackson MC, Joseph A, Jensen FE. AMPA Receptor antagonist NBQX attenuates later-life epileptic seizures and autistic-like social deficits following neonatal seizures. Epilepsia. 2013; 54:1922–1932. [PubMed: 24117347]

Lisman JE. Three Ca2+ levels affect plasticity differently: the LTP zone, the LTD zone and no man's land. J Physiol. 2001; 532:285. [PubMed: 11306649]

Malenka RC, Bear MF. LTP and LTD: an embarrassment of riches. Neuron. 2004; 44:5–21. [PubMed: 15450156]

Malenka RC, Kauer JA, Perkel DJ, Nicoll RA. The impact of postsynaptic calcium on synaptic transmission--its role in long-term potentiation. Trends Neurosci. 1989; 12:444–450. [PubMed: 2479146]

Mammen AL, Kameyama K, Roche KW, Huganir RL. Phosphorylation of the alpha-amino-3-hydroxy-5-methylisoxazole4-propionic acid receptor GluR1 subunit by calcium/calmodulin-dependent kinase II. J. Biol. Chem. 1997; 272:32528–32533. [PubMed: 9405465]

Man HY. GluA2-lacking, calcium-permeable AMPA receptors--inducers of plasticity? Curr Opin Neurobiol. 2011; 21:291–298. [PubMed: 21295464]

Manning SM, Boll G, Fitzgerald E, Selip DB, Volpe JJ, Jensen FE. The clinically available NMDA receptor antagonist, memantine, exhibits relative safety in the developing rat brain. International Journal of Developmental Neuroscience. 2011; 29:767–773. [PubMed: 21624454]

Minchom P, Niswander K, Chalmers I, Dauncey M, Newcombe R, Elbourne D, Mutch L, Andrews J, Williams G. Antecedents and outcome of very early neonatal seizures in infants born at or after term. Br J Obstet Gynaecol. 1987; 94:431–439. [PubMed: 3580326]

Neyman S, Manahan-Vaughan D. Metabotropic glutamate receptor 1 (mGluR1) and 5 (mGluR5) regulate late phases of LTP and LTD in the hippocampal CA1 region in vitro. Eur J Neurosci. 2008; 27:1345–1352. [PubMed: 18364018]

Nie D, Di Nardo A, et al. Tsc2-Rheb signaling regulates EphA-mediated axon guidance. Nat Neurosci. 2010; 13:163–172. [PubMed: 20062052]

Okabe S, Collin C, Auerbach JM, Meiri N, Bengzon J, Kennedy MB, Segal M, McKay RD. Hippocampal synaptic plasticity in mice overexpressing an embryonic subunit of the NMDA receptor. J Neurosci. 1998; 18:4177–4188. [PubMed: 9592097]

Oliet SH, Malenka RC, Nicoll RA. Two distinct forms of long-term depression coexist in CA1 hippocampal pyramidal cells. Neuron. 1997; 18:969–982. [PubMed: 9208864]

Pandey SP, Rai R, Gaur P, Prasad S. Development- and age-related alterations in the expression of AMPA receptor subunit GluR2 and its trafficking proteins in the hippocampus of male mouse brain. Biogerontology. 2015; 16:317–328. [PubMed: 25559403]

Pellegrini-Giampietro DE, Bennett MVL, Zukin RS. Are Ca 2+ -permeable kainate/AMPA receptors more abundant in immature brain? Neuroscience Letters. 1992; 144:65–69. [PubMed: 1331916]

Rajasekaran K, Todorovic M, Kapur J. Calcium-permeable AMPA receptors are expressed in a rodent model of status epilepticus. Ann Neurol. 2012; 72:91–102. [PubMed: 22829271]

Rakhade SN, Klein PM, Huynh T, Hilario-Gomez C, Kosaras B, Rotenberg A, Jensen FE. Development of later life spontaneous seizures in a rodent model of hypoxia-induced neonatal seizures. Epilepsia. 2011; 52:753–765. [PubMed: 21366558]

Rakhade SN, Zhou C, Aujla PK, Fishman R, Sucher NJ, Jensen FE. Early alterations of AMPA receptors mediate synaptic potentiation induced by neonatal seizures. J Neurosci. 2008; 28:7979–7990. [PubMed: 18685023]

Rozov A, Sprengel R, Seeburg PH. GluA2-lacking AMPA receptors in hippocampal CA1 cell synapses: evidence from gene-targeted mice. Front Mol Neurosci. 2012; 5:22. [PubMed: 22375105]

Sanchez RM, Dai W, Levada RE, Lippman JJ, Jensen FE. AMPA/kainate receptor-mediated downregulation of GABAergic synaptic transmission by calcineurin after seizures in the developing rat brain. J. Neurosci. 2005; 25:3442–3451. [PubMed: 15800199]

Sanchez RM, Koh S, Rio C, Wang C, Lamperti ED, Sharma D, Corfas G, Jensen FE. Decreased glutamate receptor 2 expression and enhanced epileptogenesis in immature rat hippocampus after perinatal hypoxia-induced seizures. J Neurosci. 2001; 21:8154–8163. [PubMed: 11588188]

Sanderson JL, Gorski JA, Dell'Acqua ML. NMDA Receptor-Dependent LTD Requires Transient Synaptic Incorporation of Ca(2+)-Permeable AMPARs Mediated by AKAP150-Anchored PKA and Calcineurin. Neuron. 2016; 89:1000–1015. [PubMed: 26938443]

Schmued LC, Hopkins KJ. Fluoro-Jade B: a high affinity fluorescent marker for the localization of neuronal degeneration. Brain Res. 2000; 874:123–130. [PubMed: 10960596]

Seidenman KJ, Steinberg JP, Huganir R, Malinow R. Glutamate receptor subunit 2 Serine 880 phosphorylation modulates synaptic transmission and mediates plasticity in CA1 pyramidal cells. J Neurosci. 2003; 23:9220–9228. [PubMed: 14534256]

Shouval HZ, Bear MF, Cooper LN. A unified model of NMDA receptor-dependent bidirectional synaptic plasticity. Proc Natl Acad Sci U S A. 2002; 99:10831–10836. [PubMed: 12136127]

Silverstein FS, Jensen FE. Neonatal seizures. Ann Neurol. 2007; 62:112–120. [PubMed: 17683087]

Stevens CF, Wang Y. Changes in reliability of synaptic function as a mechanism for plasticity. Nature. 1994; 371:704–707. [PubMed: 7935816]

Steward O, Falk PM. Selective localization of polyribosomes beneath developing synapses: a quantitative analysis of the relationships between polyribosomes and developing synapses in the hippocampus and dentate gyrus. J Comp Neurol. 1991; 314:545–557. [PubMed: 1814974]

Sun H, Kosaras B, Klein PM, Jensen FE. Mammalian target of rapamycin complex 1 activation negatively regulates Polo-like kinase 2-mediated homeostatic compensation following neonatal seizures. Proc Natl Acad Sci U S A. 2013

Talos DM, Sun H, Zhou X, Fitzgerald EC, Jackson MC, Klein PM, Lan VJ, Joseph A, Jensen FE. The Interaction Between Early Life Epilepsy and Autistic-Like Behavioral Consequences: A Role for the Mammalian Target of Rapamycin (mTOR) Pathway. PLoS One. 2012; 7:e35885. [PubMed: 22567115]

Tanaka M, Sakata S, Hirashima N. Effects of 1-naphthyl acetyl spermine on dendrite formation by cultured cerebellar Purkinje cells. Neurosci Lett. 2009; 462:30–32. [PubMed: 19560511]

Tsubokawa H, Oguro K, Masuzawa T, Nakaima T, Kawai N. Effects of a spider toxin and its analogue on glutamate-activated currents in the hippocampal CA1 neuron after ischemia. J Neurophysiol. 1995; 74:218–225. [PubMed: 7472325]

Turrigiano G. Homeostatic synaptic plasticity: local and global mechanisms for stabilizing neuronal function. Cold Spring Harb Perspect Biol. 2012; 4:a005736. [PubMed: 22086977]

Twele F, Bankstahl M, Klein S, Romermann K, Loscher W. The AMPA receptor antagonist NBQX exerts anti-seizure but not antiepileptogenic effects in the intrahippocampal kainate mouse model of mesial temporal lobe epilepsy. Neuropharmacology. 2015; 95:234–242. [PubMed: 25839899]

Volpe JJ, Kinney HC, Jensen FE, Rosenberg PA. The developing oligodendrocyte: key cellular target in brain injury in the premature infant. Int J Dev Neurosci. 2011; 29:423–440. [PubMed: 21382469]

Washburn MS, Numberger M, Zhang S, Dingledine R. Differential dependence on GluR2 expression of three characteristic features of AMPA receptors. J. Neurosci. 1997; 17:9393–9406. [PubMed: 9390995]

Wirrell EC, Grossardt BR, Wong-Kisiel LC, Nickels KC. Incidence and classification of new-onset epilepsy and epilepsy syndromes in children in Olmsted County, Minnesota from 1980 to 2004: a population-based study. Epilepsy Res. 2011; 95:110–118. [PubMed: 21482075]

Yang SN, Tang YG, Zucker RS. Selective induction of LTP and LTD by postsynaptic [Ca2+]i elevation. J Neurophysiol. 1999; 81:781–787. [PubMed: 10036277]

Yang Y, Wang XB, Zhou Q. Perisynaptic GluR2-lacking AMPA receptors control the reversibility of synaptic and spines modifications. Proc Natl Acad Sci U S A. 2010; 107:11999–12004. [PubMed: 20547835]

Yuan T, Bellone C. Glutamatergic receptors at developing synapses: the role of GluN3A-containing NMDA receptors and GluA2-lacking AMPA receptors. Eur J Pharmacol. 2013; 719:107–111. [PubMed: 23872415]

Zhao Q, Hu Y, Holmes GL. Effect of topiramate on cognitive function and activity level following neonatal seizures. Epilepsy & Behavior. 2005; 6:529–536. [PubMed: 15878305]

Zhou C, Lippman Bell JJ, Sun H, Jensen FE. Hypoxia-induced neonatal seizures diminish silent synapses and long-term potentiation in hippocampal CA1 neurons. J Neurosci. 2011; 13:18211–18222.

Highlights

- Neonatal seizures enhance cellular Ca2+ response within 48 hours.
- Altered Ca2+ is temporally associated with decreased synaptic CP-AMPARs and attenuated LTD
- *In vivo* AMPAR antagonist treatment prevents the post-seizure changes.
- May provide a mechanism contributing to behavioral and plasticity deficits in this model

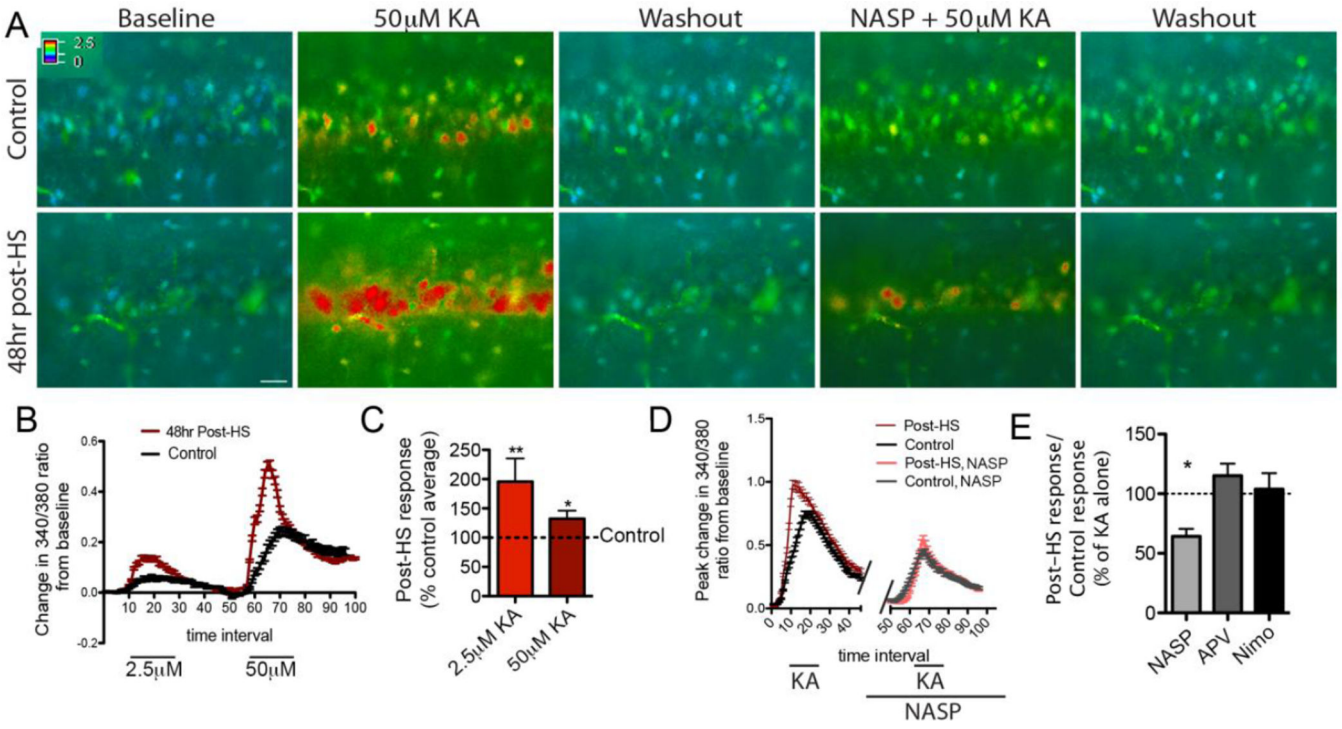

Figure 1. Peak Ca^{2+} response to KA increases 48 hours post-HS and is mediated by CP-AMPARs

A) Time-lapse ratiometric fura-2 imaging in CA1 in slices from post-HS (bottom) and littermate control (top) rats demonstrating the change in 340/380 ratios in response to KA before and after incubation with NASP; Bar= 30μm. B) Example of 340/380 ratios in response to 2.5 and 50μM KA in multiple cells averaged in one post-HS (red) and one control slice (black). C) Quantification of peak change in 340/380 ratio shows that response to 2.5 or 50μM KA is significantly higher in CA1 pyramidal neurons 48 hours post-HS (mean response to 2.5μM KA=0.23±0.05, n=6 rats; response to 50μM KA=0.67±0.07, n=10 rats) than in controls (2.5μM KA=0.12±0.02, n=6 rats, p=0.01 by repeated measures ANOVA, 50μM KA=0.51±0.07, n=10 rats p=0.049 by repeated measures ANOVA), represented together here as a percent of the control average indicated by the dotted line. D) Quantification of change in 340/380 ratio from baseline in multiple cells from one control (black) and one 48 hours post-HS slice (red) before and after NASP treatment; n=7 slices/group, p=0.02 by t-test. E) Quantification of peak responses with and without NASP, APV and nimodipine as a ratio of post-HS responses to that of littermate controls illustrates that NASP, but not APV or nimodipine render equivalent peak Ca^{2+} responses to KA from cells in post-HS and controls (n=5–8 slices/group; see text). Data is represented as mean±SE.

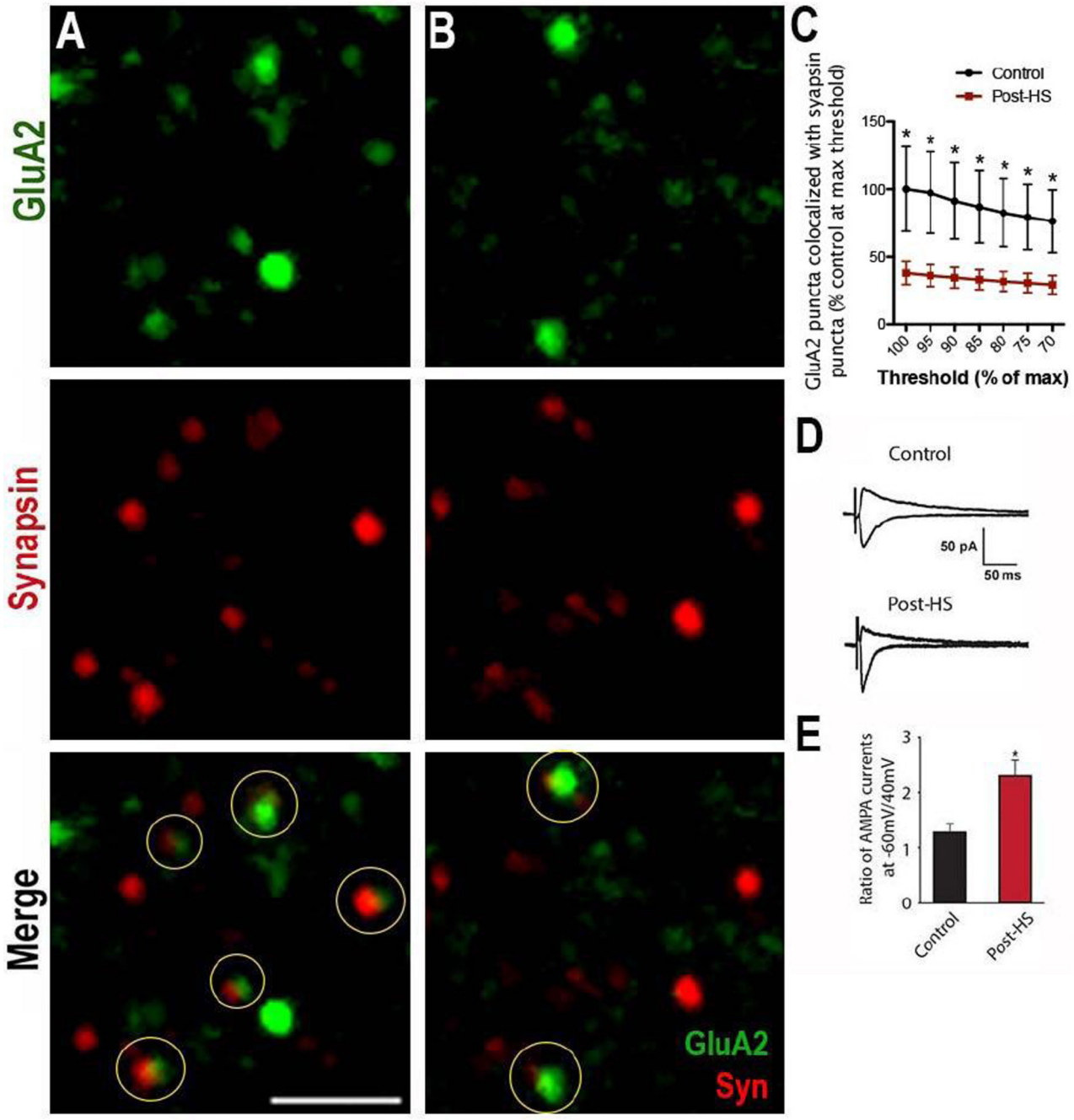

Figure 2. Surface GluA2 expression decreases 48 hours post-HS

A, B) Immunohistochemistry of surface GluA2 (green) and synapsin (red) in (A) control and (B) post-HS in CA1 s. radiatum of the hippocampus of P12 Long-Evans rats 48 hours post-HS. Circles highlight colocalization; Bar=2μm. C) Quantification shows a significant decrease in surface GluA2/Synapsin colocalization in post-HS rats compared to controls over multiple thresholds represented as a percentage of the control at each threshold; post-HS n=11 fields from 6 rats; control=8 fields from 5 rats; p=0.04 by t-test of control vs. HS at each threshold. D) Averaged traces of AMPAR eEPSCs at −60 and +40 mV while blocking

NMDARs and GABARs show that rectification increases post-HS. E) Summary of AMPAR eEPSC ratio at −60 mV to +40 mV; n=5 control and 6 post-HS, p=0.014 by t-test. Data is represented as mean±SE.

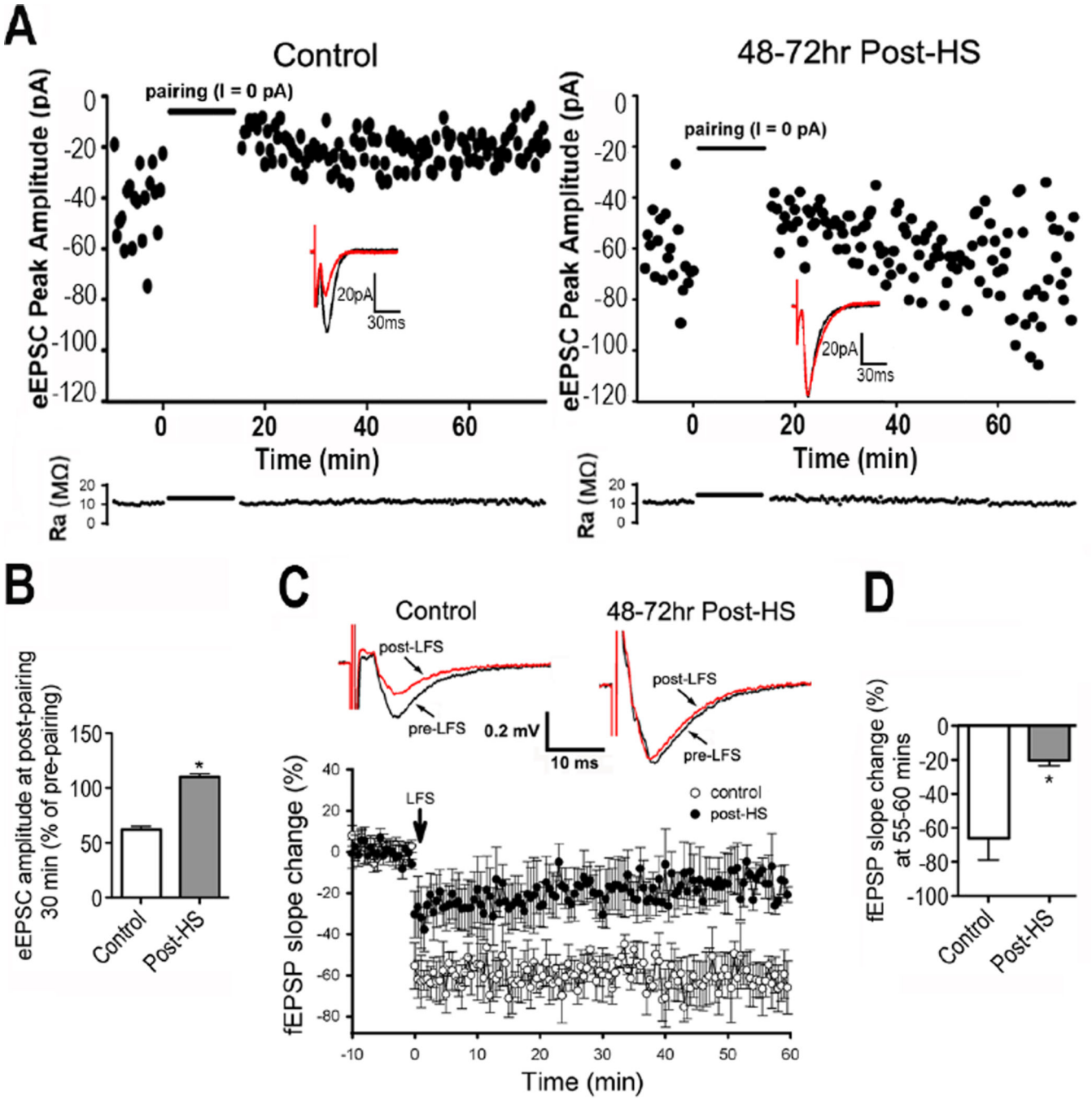

Figure 3. LTD is attenuated 48 hours post-HS

A) Time course of eEPSC amplitude in CA1 pyramidal neurons with pairing protocol shows attenuation in LTD 48–72 hours post-HS (right) compared with control (left). Inserts are representative traces before and 30 min post-LFS. Lower panel shows the time course of access resistance during LTD recording period. B) Summarized eEPSC amplitude changes in slices before pairing and 30 min post-pairing for control and post-HS rats; n=6 slices/group, p=0.02 by t-test. C) Representative averaged field (f)EPSP traces recorded in CA1 pyramidal neurons from control (top left panel) and post-seizures (*in vivo* seizures at P10)

(Top right panel). Time course of LFS induced fEPSP change shows attenuated LTD in slices from rats post-HS compared to controls (lower panel). D) Quantification of fEPSP slope percent change from pre-LFS averaged over minutes 55–60 post-LFS in slices taken 48–72 hours post-HS and from age-matched controls (n=6, p=0.006 by t-test). Slopes were significantly lower in controls than in post-HS slices. Data is represented as mean±SE.

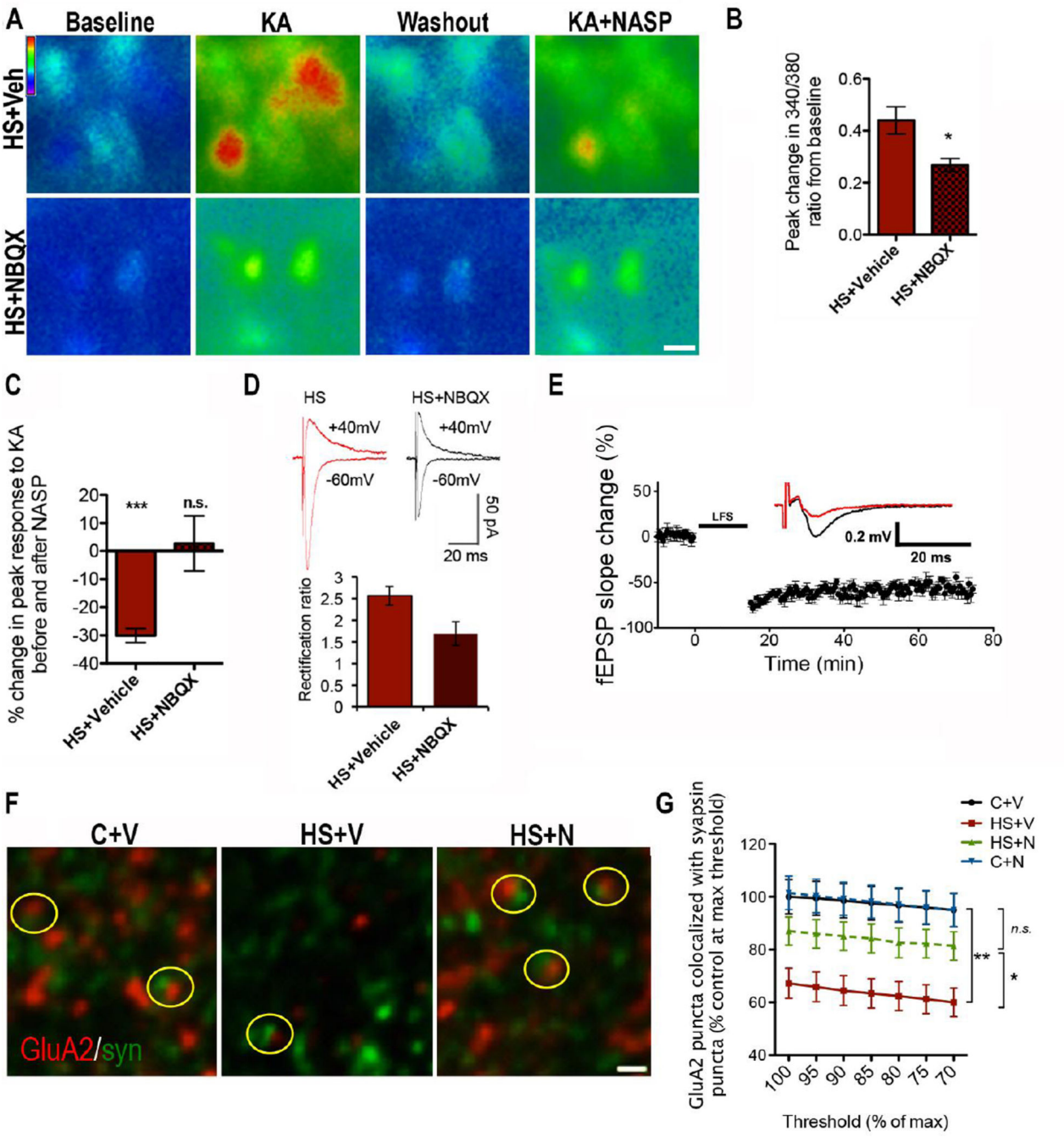

Figure 4. Post-HS NBQX treatment restores normal GluA2 expression, Ca^{2+}response, LTD and CP-AMPAR function at 48 hours post-HS

A) Ratiometric fura-2 imaging in CA1 pyramidal neurons of Ca^{2+} response to 50μM KA (followed by washout) in slices from HS+V (top) or HS+N rats (bottom), shows that NBQX lowers the peak response. NASP effect is dampened in NBQX treated animals compared to controls; Bar=10μm. B) Quantification of peak change in Ca^{2+} response, measured by 340/380 ratio, from cells averaged per slice from pairs of littermate rats treated with vehicle or NBQX; n=11 slices from 8 rats/group, p=0.01 by Mann Whitney test. D) Quantification of Ca^{2+} imaging demonstrates that NASP has minimal effect on KA response in slices from

HS+N rats, in contrast to slices from HS+V rats; HS+V, n=6 slices from 4 animals; 8–19 cells/slice, $p<0.0001$ by one-sample t-test, HS+N n=6 slices from 4 animals/group; 10–26 cells/slice, $p=0.79$ by one-sample t-test. D) In brain slices adjacent to those used in C, rectification is higher in slices from HS+N rats compared to HS+V; HS+V n=8; HS+N n=7, $p=0.024$ by t-test. E) Time course of LFS induced fEPSP attenuation for HS+N is similar to LTD in controls. Arrow marks the start of tetanus stimulation. Inset is representative averaged fEPSP traces where black=pre-LFS and red=60 min post-LFS; HS+N n=8, $p=0.331$ vs. controls by t-test, $p=0.001$ vs. HS+V by t-test. Data is represented as mean±SE. F) GluA2 and synapsin staining in *s. radiatum* of hippocampal CA1 of P12 rats from the following conditions (left to right): P12 control treated with vehicle (C+V), 48 hours post-HS treated with vehicle (HS+V), and 48hr post-HS treated with 20mg/kg NBQX (HS+N). Yellow circles highlight colocalization. Images are maximum projections of 3 z-planes. Bar=0.5μm. G) Quantification of colocalized GluA2/synapsin puncta at multiple thresholds of GluA2 staining intensity, expressed as percentage of vehicle-treated controls, shows that NBQX treatment prevents the decrease in GluA2 synaptic expression. (HS+N and HS+V n=14 fields from 6 rat, C+V n=11 fields from 5 rats, C+N n=7 fields from 4 rats; at each threshold, $p<0.001$ by ANOVA for all 4 groups; with Bonferroni post-hoc test, $p<0.05$ for HS+V vs. HS+N; $p>0.05$ for C+V vs. HS+N, $p>0.05$ for C+V vs. C+N, and $p<0.01$ for C+V vs. HS+V).